

## Recent development of $\text{LiNi}_x\text{Co}_y\text{Mn}_z\text{O}_2$ : Impact of micro/nano structures for imparting improvements in lithium batteries

Cheng-chi PAN<sup>1</sup>, Craig E. BANKS<sup>2</sup>, Wei-xin SONG<sup>1</sup>, Chi-wei WANG<sup>3</sup>, Qi-yuan CHEN<sup>1</sup>, Xiao-bo JI<sup>1</sup>

1. Key Laboratory of Resources Chemistry of Nonferrous Metals, Ministry of Education, College of Chemistry and Chemical Engineering, Central South University, Changsha 410083, China;

2. Faculty of Science and Engineering, School of Biology, Chemistry and Health Science, Division of Chemistry and Materials, Manchester Metropolitan University, Chester Street, Manchester M1 5GD, Lancs, UK;

3. Tianjin EV Energies Company Limited, Tianjin 300380, China

Received 10 October 2012; accepted 10 December 2012

**Abstract:** The recent advancement in the design, synthesis, and fabrication of micro/nano structured  $\text{LiNi}_x\text{Co}_y\text{Mn}_z\text{O}_2$  with one-, two-, and three-dimensional morphologies was reviewed. The major goal is to highlight  $\text{LiNi}_x\text{Co}_y\text{Mn}_z\text{O}_2$  materials, which have been utilized in lithium ion batteries with enhanced energy and power density, high energy efficiency, superior rate capability and excellent cycling stability resulting from the doping, surface coating, nanocomposites and nano-architecturing.

**Key words:** lithium-ion battery; micro/nano structures;  $\text{LiNi}_x\text{Co}_y\text{Mn}_z\text{O}_2$ ; doping; surface coating; composite materials

### 1 Introduction

Clean energy sources have become an ever increasing and urgent demand in the fast-growing market for portable electronic devices and the development of hybrid electric vehicles. Since renewable and sustainable sources will usher in a long-anticipated transition away from fossil fuels in the coming decades, highly efficient and advanced energy conversion and storage devices, such as lithium-ion batteries (LIBs), which are most convenient and portable form of electrical energy storage, have become essential requirements. LIBs have numerous outstanding features including high energy density, high conversion efficiency, no gaseous exhaust, improved safety and longer cycle life. The research and promotion of cathode materials are most important in the application potential of LIBs. The application of batteries utilizing layered  $\text{LiCoO}_2$  has been limited by the relatively low specific capacity and high cost of cobalt application in plug-in hybrid vehicles (PHEVs) and all-electric vehicles (EVs). Additionally, despite the abundance of iron and manganese, olivine  $\text{LiFePO}_4$  and

spinel  $\text{LiMn}_2\text{O}_4$  do not exhibit a high enough gravimetric and volumetric energy density for transportation applications and as such are not likely adequate candidates. However, lithium nickel cobalt manganese oxides have been investigated as advanced positive electrode materials for lithium-ion batteries designated to power PHEVs and EVs.

There are some problems and drawbacks in the existing Li-ion batteries, for instance, phase transformation, deterioration in microstructure or architecture of the electrodes associated with volume expansion or contraction, and morphology change of the active electrode materials during cycling. The development of nanoscience and nanotechnology has provided the possibility to tailor the physicochemical properties and improve the performance of functional materials; to some extent, nanostructured materials will be helpful to solve these issues [1,2]. In fact, the development of nanostructured materials has become a very active research field in the areas of Li-ion batteries. There are five dominating unique advantages in nanostructured electrodes for Li batteries [3], which are large surface area (or surface to volume ratio), short

**Foundation item:** Projects (51134007, 21003161, 21250110060) supported by the National Natural Science Foundation of China; Project (11MX10) supported by Central South University Annual Mittal-Founded Innovation Project; Project (2011ssxt086) supported by Fundamental Research Funds for the Central Universities, China

**Corresponding author:** Xiao-bo JI; Tel: +86-731-88879616; Fax: +86-731-88879616; E-mail: [xji@csu.edu.cn](mailto:xji@csu.edu.cn)  
DOI: 10.1016/S1003-6326(13)62436-X

diffusion length, enhanced ionic and electronic conductivity, improved mechanical strength and structural integrity, and hierarchical architecture of nano-porous structures. Although nanomaterials tend to form agglomerates, they can be mitigated through properly designing the nanostructure and fabrication process. Therefore, micro/nano structured anodes based on  $\text{LiNi}_x\text{Co}_y\text{Mn}_z\text{O}_2$  will be an effective strategy to enable a breakthrough to overcome these problems experienced by present technologies.

Manipulation of micro/nano structured electrode materials can provide versatile strategies toward improving the electrochemical properties. Many recent review articles [4–7] have summarized that the nanostructural electrode materials are able to manifest higher capacities, better rate capabilities, superior cycling performance and thermal stability compared with their bulk counterparts.

In this feature article, we will give an overview concentrating on  $\text{LiNi}_x\text{Co}_y\text{Mn}_z\text{O}_2$  based cathode materials to highlight various constructed nanostructures including 2-D nanosheets, nanocomposites, novel hollow and core-shell structures, and complex hierarchical 3-D nanostructures. We also discuss the rational design and synthesis of unique nanostructures, and its beneficial effects of proper nanostructuring and advanced compositing on enhanced physicochemical properties of these electrode materials.

## 2 Structure and characterization

LIU et al [8] reported the synthesis of  $\text{LiNi}_{1-x-y}\text{Co}_x\text{Mn}_y\text{O}_2$  ( $0 \leq x \leq 0.5$ ,  $0 \leq y \leq 0.3$ ), using the partial substitution of Ni by Co and Mn in  $\text{LiNiO}_2$ . Such structures, which can be utilized as cathode materials in lithium batteries, have gradually been adopted by researchers. The structures of  $\text{LiNi}_x\text{Co}_y\text{Mn}_z\text{O}_2$  [9–11] (Fig. 1) are basically the same as that of  $\alpha\text{-NaFeO}_2$  layered  $\text{LiCoO}_2$ , which is a well-defined layer structure based on a hexagonal  $\alpha\text{-NaFeO}_2$  structure with space group of  $R\bar{3}m$ , in which Li and O mainly occupy the  $3a$  and  $6c$  sites in a  $\text{MO}_6$  octahedron respectively, and Co, Ni, and Mn randomly or non-randomly occupy the  $3b$  site in transition metal ion distributions [12,13], one of which is sensitive to the preparation procedure [14].

In these  $\text{LiNi}_x\text{Co}_y\text{Mn}_z\text{O}_2$  compounds, nickel, cobalt and manganese are adjacent elements on the periodic table, in which the valences of transition metal elements exhibit generally complicated. Co is usually 2, Ni has mixed valence and Mn may be 2, 3, or 4, while the variation of valence is helpful to complete understanding of the charge-discharge mechanism [15]. The intercalation and de-intercalation of lithium ions in aqueous solution follows an almost similar mechanism in

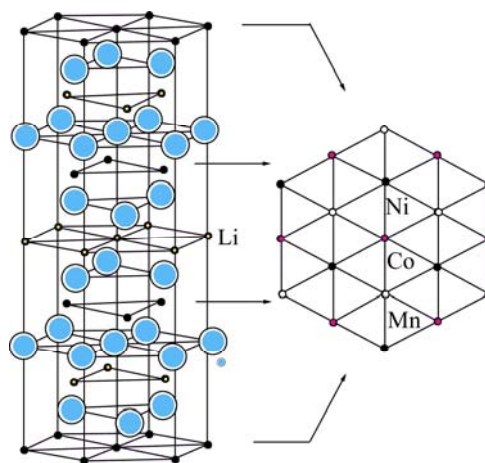


Fig. 1 Structural model of  $\text{LiNi}_{1/3}\text{Co}_{1/3}\text{Mn}_{1/3}\text{O}_2$

non-aqueous systems [16].

Co incorporation may be effective to enhance its layered structural stability and suppress transition metal ion migration into the Li sites [17], where the  $\text{Ni}^{2+}$  and  $\text{Li}^+$  cations occupy each other's sites, meanwhile, prevent phase transformation and improve its electrical conductivity. However, the increase of Co content results in a decrease of the lattice parameter of  $c$  and  $a$ , and an increase of the  $c/a$  ratio, leading to a decrease of the lattice cell with a reduction in specific capacity. Note that the cobalt induces significant structural transformation during cycling in the high-potential range [18], and the slightly higher content of cobalt is necessary to achieve better cycle life.

Moreover, Ni ions can avoid electrolyte decomposition [19,20] at the end of the charge potential and are beneficial to Li diffusion, whereas the existence of Mn ions may hinder Li motion by increasing the activation energy [21,22]. Nevertheless, the increase of Ni content results in an increase of lattice parameters of  $c$  and  $a$ , and a decrease of the  $c/a$  ratio, leading to an increase of the lattice cell with an improvement in the reversible specific capacity [23]. However, the high content of Ni leads to cation mixing, since the radius of  $\text{Ni}^{2+}$  (0.069 nm) is close to that of  $\text{Li}^+$  (0.076 nm), partial  $\text{Ni}^{2+}$  may occupy  $3a$  sites and then cause cation mixing and exhibit remarkable irreversible initial capacities. Furthermore,  $\text{Ni}^{3+}$  and  $\text{Ni}^{4+}$  produced during charging may cause the collapse of the layer structure locally, resulting in the degradation of electrochemical performances.

The partial substitution of Ni by Mn can improve the safety and thermal stabilities [24], while Mn is inactive to help maintain structural stability of the  $\alpha\text{-NaFeO}_2$  phase [25]. With increasing the substitution of Mn ions for Ni ions, the lattice parameter  $a$  decreases, while the lattice parameters  $c$  and  $c/a$  increase [26]. Superfluous Mn can lead to a phase transition from a layered structure to a spinel one. Therefore, the contents

of Ni, Co, and Mn need to be optimized for the best performance of the materials [27].

### 3 Preparation and performance

The different synthesis methodologies of micron- and nano-structured  $\text{LiNi}_x\text{Co}_y\text{Mn}_z\text{O}_2$  have a distinct effect upon their electrochemical performances, and as such, the synthesis of  $\text{LiNi}_x\text{Co}_y\text{Mn}_z\text{O}_2$  with controllable morphology and size has drawn intensive research attention. Synthesis approaches mainly include high temperature solid-state method, co-precipitation synthesis, sol–gel method, microwave-hydrothermal synthesis, molten salt method, spray drying method, etc.

#### 3.1 Solid state method

Solid-state synthesis is the most common method for the preparation of nanometer sized  $\text{LiNi}_x\text{Co}_y\text{Mn}_z\text{O}_2$  in industrial produces due to the simplicity of required equipment and easy to control processes. However, the disadvantages to the approaches are the mechanical requirement needed to refine and mix raw materials, and it is difficult to obtain homogeneous distributions of the product, which can significantly influence the electrochemical properties. OHZUKU and MAKIMURA [28] first synthesized the layered  $\text{LiCo}_{1/3}\text{Ni}_{1/3}\text{Mn}_{1/3}\text{O}_2$  cathode material at 1000 °C for 15 h in air, using  $\text{LiOH}\cdot\text{H}_2\text{O}$ ,  $\text{CoCO}_3$  and a nickel manganese hydroxide as raw materials. The rechargeable capacity was found to be more than 200 mA·h/g with little capacity fading, such that it could be cycled in the voltage range of 3.5–4.2 V with a rechargeable capacity of 150 mA·h/g. Due to a complex solid solution mechanism, the operating voltage of  $\text{Li}/\text{LiCo}_{1/3}\text{Ni}_{1/3}\text{Mn}_{1/3}\text{O}_2$  was found to be 0.2 V lower than that of a cell with just  $\text{LiCoO}_2$ . TAN and LIU [29] prepared  $\text{LiNi}_{1/3}\text{Co}_{1/3}\text{Mn}_{1/3}\text{O}_2$  with a size of 150–200 nm at a suitable temperature of 900 °C using  $\alpha\text{-MnO}_2$  nanorods as the raw material, which exhibited small and uniform particles due to highly ordered layer structure and lower degree of cation mixing. This material was found to exhibit excellent cycling performances and 93.9% of an initial capacity retention after 30 cycles between 2.5 and 4.5 V. DOU and WANG [30] reported that a series of  $\text{LiNi}_{0.5-x}\text{Mn}_{0.5-x}\text{Co}_{2x}\text{O}_2$  ( $0 < 2x \leq 0.33$ ) compounds with single phase were prepared by solid-state reaction using Ni–Mn–Co oxide precursor.  $\text{LiNi}_{0.475}\text{Mn}_{0.475}\text{Co}_{0.05}\text{O}_2$  presented the best electrochemical performance with a capacity of 168 mA·h/g in the voltage range of 2.5–4.4 V and 86.1% of initial capacity retention over 50 cycles among the samples, while  $\text{LiNi}_{0.34}\text{Mn}_{0.33}\text{Co}_{0.33}\text{O}_2$  showed high rate capacity at a current rate of 1000 mA/g and stable capacity about 63 mA·h/g.

#### 3.2 Precipitation method

Precipitation synthesis is the most popular approach to acquire  $\text{LiNi}_x\text{Co}_y\text{Mn}_z\text{O}_2$  with special morphologies. The key to the method is the preparation process for the precursor. In virtue of molecular-level contact, the precursors have small particles and mixing uniformity. Precipitation method has many advantages, such as accurate stoichiometric proportions and a lower synthesis temperature. However, operational complexity and low reaction stability are in need of improvement.

DENG et al [31] reported that  $\text{LiNi}_{1/3}\text{Co}_{1/3}\text{Mn}_{1/3}\text{O}_2$  can be prepared by carbonate co-precipitation method using  $(\text{NH}_4)_2\text{CO}_3$  as precipitator. The sample with hexagonal layered structure had spherical particle shapes and uniform particle sizes with the diameter of the particles of about 6  $\mu\text{m}$  and a narrow particle size distribution. The initial discharge capacity was 162.8 mA·h/g and the capacity retention reached 93.6% after 100 cycles.

YANG et al [32] synthesized  $\text{Li}[\text{Ni}_{1/3}\text{Mn}_{1/3}\text{Co}_{1/3}]\text{O}_2$  via two different pretreatment processes with the  $[\text{Ni}_{1/3}\text{Co}_{1/3}\text{Mn}_{1/3}]\text{O}_4$  precursor and lithium hydroxide ( $\text{LiOH}\cdot\text{H}_2\text{O}$ ). A well-ordered layer structure product exhibited nearly the same spherical shapes as the precursor. The  $\text{Li}[\text{Ni}_{1/3}\text{Mn}_{1/3}\text{Co}_{1/3}]\text{O}_2$  material prepared by solution phase route exhibited a higher capacity retention and better rate capability. The initial discharge capacity reached 178 mA·h/g and the capacity retention was 98.7% at a current density of 20 mA/g after 50 cycles. Moreover, it delivered a high discharge capacity of 135 mA·h/g at a current density of 1000 mA/g. Shortly after, they prepared spherical  $\text{Li}[\text{Ni}_{1/3}\text{Co}_{1/3}\text{Mn}_{1/3}]\text{O}_2$  cathode materials with various microstructures by a continuous carbonate co-precipitation method using different lithium sources. The  $\text{Li}_2\text{CO}_3$  was preferable when preparing the  $\text{Li}[\text{Ni}_{1/3}\text{Co}_{1/3}\text{Mn}_{1/3}]\text{O}_2$  with high rate cycling performance, which was mainly attributed to the uniform distribution of the spherical particles. The initial discharge capacity retention reached 97.5% and 92% at 1.0C and 5.0C after 100 cycles, respectively.

HUANG et al [33] synthesized spherical  $\text{Ni}_x\text{Co}_{(1-2x)}\text{Mn}_x(\text{OH})_2$  ( $x=0.333, 0.4, 0.416, 0.45$ ) precursors with Co-rich in the core of the material and Co-poor on the surface by improved co-precipitation (Fig. 2). The well-ordered spherical  $\text{LiNi}_x\text{Co}_{(1-2x)}\text{Mn}_x\text{O}_2$  was prepared by sintering cobalt concentration-gradient precursor and  $\text{Li}_2\text{CO}_3$  at 950 °C for 16 h in air. The  $\text{LiNi}_x\text{Co}_{(1-2x)}\text{Mn}_x\text{O}_2$  materials from gradient precursor exhibited lower degree of cation disorder and better rate capability attributed to the cobalt-rich in core and cobalt concentration-gradient precursor.

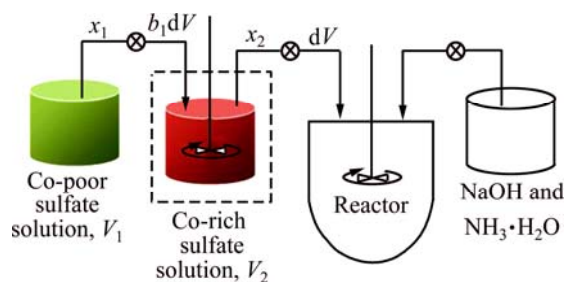


**Fig. 2** Illustration of co-precipitation process: (a)  $V_1$  is initial volume of Co-poor solution; (b)  $V_2$  is initial volume of Co-rich solution; (c)  $x_1$  is Co molar concentration of a species in Co-poor solution; (d)  $x_2$  is initial Co molar concentration of Co-rich solution fed to reactor; (e)  $V$  is volume of sulfate solution fed to reactor in time of  $t$ ; (f)  $dV$  is volume of solution fed to reactor in time of  $dt$ ; (g)  $b_1=V_1/(V_1+V_2)$

### 3.3 Hydrothermal synthesis

The hydrothermal synthesis could prepare  $\text{LiNi}_x\text{Co}_y\text{Mn}_z\text{O}_2$  powders with strong penetration ability and homogeneous morphology, and the method has many advantages, such as larger specific capacity, better cyclic stability and excellent rate capability than the traditional methods.

MYUNG et al [34] prepared a fine and spherical layered  $\text{Li}[\text{Ni}_{1/3}\text{Co}_{1/3}\text{Mn}_{1/3}]\text{O}_2$  at 800 °C in air for 5 h using  $[\text{Ni}_{1/3}\text{Co}_{1/3}\text{Mn}_{1/3}](\text{OH})_2$  synthesized as a hydrothermal precursor via a co-precipitation route. The initial discharge capacity was found to be 157 mA·h/g (4.3 V cut-off) and 182 mA·h/g (4.6 V cut-off) with superior reversibility, the efficiency between charge and discharge was close to 100 % after the first cycle.

LU and SHEN [35] prepared  $\text{LiNi}_{1/3}\text{Co}_{1/3}\text{Mn}_{1/3}\text{O}_2$  powders by microwave-hydrothermal synthesis. The submicron particles of 1–3  $\mu\text{m}$  exhibited a less-agglomerated morphology and narrowed size distribution. When the microwave radiation temperature was 180 °C, the  $\text{LiNi}_{1/3}\text{Co}_{1/3}\text{Mn}_{1/3}\text{O}_2$  showed a high lithium-ion diffusion coefficient and good rate capability with a discharge capacity of approximately 170 mA·h/g and 98.5% of the retention capacity after 10 cycles.

XIE et al [36] prepared the ultrafine powders of  $\text{LiNi}_{1/3}\text{Co}_{1/3}\text{Mn}_{1/3}\text{O}_2$  via the mild hydrothermal method. The powders were composed of nanosized crystallites with uniform shapes and exhibited a mean crystal size of about 10 nm. WU et al [37] synthesized the layered  $\text{LiNi}_{1/3}\text{Co}_{1/3}\text{Mn}_{1/3}\text{O}_2$  materials with good crystallinity via a novel hydrothermal method followed by a short calcination process at 850 °C for 6 h, in which the  $\text{Ni}_{1/3}\text{Co}_{1/3}\text{Mn}_{1/3}(\text{OH})_2$  precursor was treated with excess amount of LiOH aqueous solution at 160 °C. The materials exhibited an initial discharge capacity of 187.7 mA·h/g at a current density of 20 mA/g and a capacity retention of 97.9% with good reversible de-intercalation

and intercalation of  $\text{Li}^+$  ions at the end of 40 cycles at discharge rate 1.0C, which was attributed to the uniform particle morphology of the materials.

### 3.4 Sol-gel method

The sol-gel method is a common way with intimate mixing at the atomic level, resulting in a compositionally homogeneous product with a narrow particle size distribution and a controlled morphology. It has the detriment of industrial production because of relatively complex synthesis process and greater environmental contamination. SHAJU and BRUCE [38] reported macro-porous  $\text{LiNi}_{1/3}\text{Co}_{1/3}\text{Mn}_{1/3}\text{O}_2$  with individual particles of narrow size distribution. The size of particles was in the range of 0.5 to 1.0  $\mu\text{m}$  and agglomerates from around 1 to 5  $\mu\text{m}$ . The first discharge capacity was 209 mA·h/g and the capacity of  $\text{LiNi}_{1/3}\text{Co}_{1/3}\text{Mn}_{1/3}\text{O}_2$  was about 190 mA·h/g at a current density of 100 mA/g with the capacity retention of 99.99% per cycle from cycle 20 to cycle 220. The material had excellent charge and discharge rates with 2244 W·h/L at 1.0C and 2008 W·h/L at 10.0C rates, respectively.

HUANG et al [39] reported that the  $\text{LiNi}_{1/3}\text{Co}_{1/3}\text{Mn}_{1/3}\text{O}_2$  (NCM) nanoparticles with a novel 1-D porous structure were synthesized by a modified sol-gel method (Fig. 3). The electrochemical activities and cyclic stability of the NCM particles had been improved by the stepwise heating/cooling crystallization process. The single crystal particle size varied widely between 150 and 600 nm for all NCMs, and the majority of pores were smaller than 80 nm, thereby, the highly porous structure with a large specific surface area gave rise to improved electrochemical activities as confirmed by the high capacity and high rate capability with excellent cyclic stability. The initial charge/discharge specific capacities of Li/M-NCM-1 and M-NCM-2 (Fig. 4) were 201.0/169.9 mA·h/g and 202.0/173.1 mA·h/g at 0.1C (20 mA/g) between 2.8 and 4.4 V, respectively. The capacity retention ratios were 86.1% and 88.7% after 50 cycles, respectively.

NITHYA et al [40] prepared  $\text{LiNi}_x\text{Co}_y\text{Mn}_z\text{O}_2$  with tartaric acid assisted sol-gel method. The well crystalline submicron particles showed the size of 0.5–1  $\mu\text{m}$ . In the voltage range of 2.7–4.9 V, the discharge capacity of  $\text{LiNi}_{0.4}\text{Co}_{0.1}\text{Mn}_{0.5}\text{O}_2$  exhibited 192 mA·h/g at 0.2C over the 50 cycles.

### 3.5 Spray drying method

The spray drying method can obtain excellent performance  $\text{LiNi}_{1/3}\text{Co}_{1/3}\text{Mn}_{1/3}\text{O}_2$  with fine and homogeneous powders and satisfactory morphology, and it is an effective way to prepare multiple complex oxides owing to lower temperature and relatively short time.

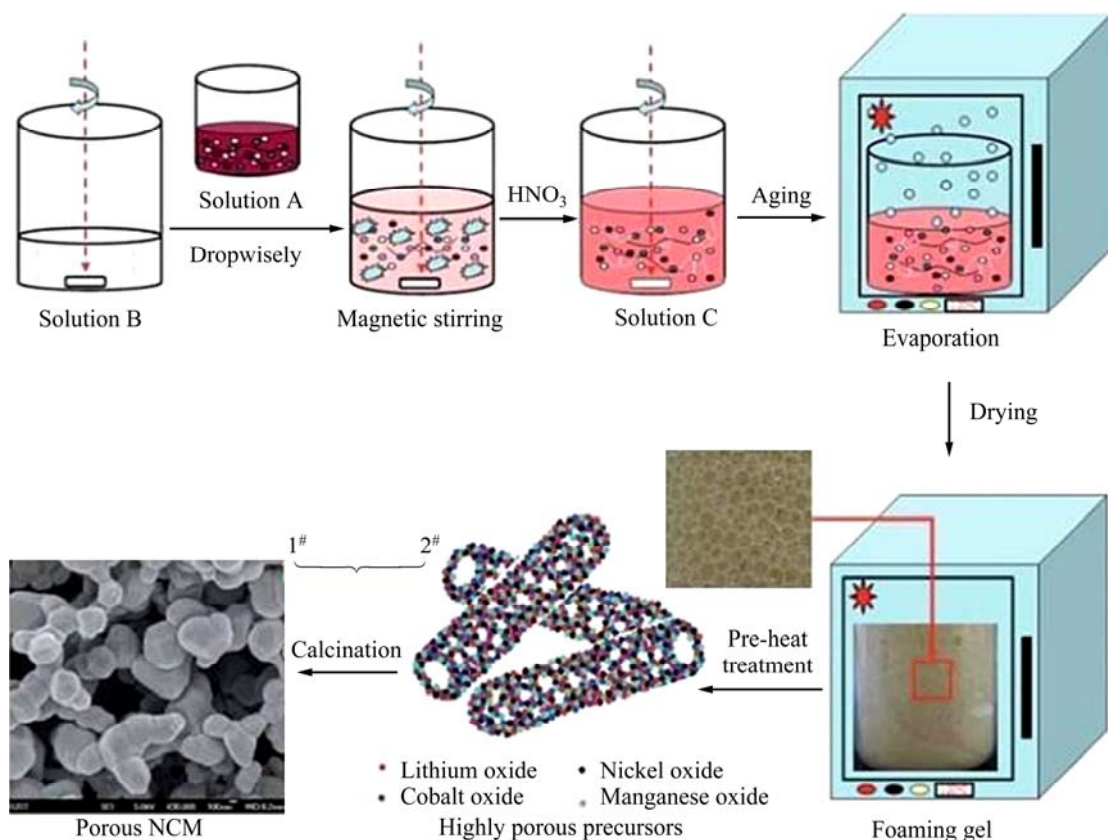


Fig. 3 Schematic illustration of M-NCMs prepared by modified sol-gel method (1<sup>#</sup> and 2<sup>#</sup> are different crystallization of M-NCMs)

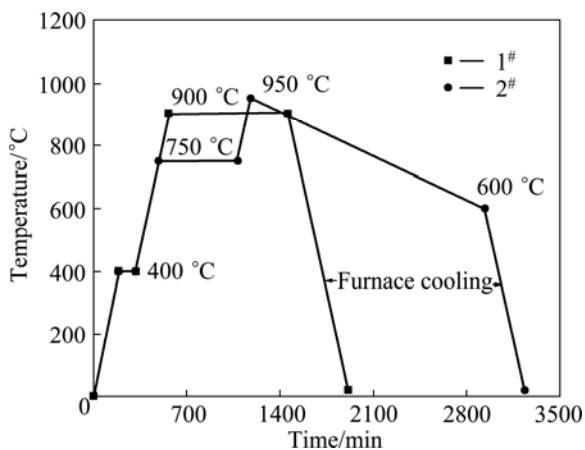


Fig. 4 Temperature–time histories employed for crystallization of NCM particles (M-NCM modified NCM, M-NCM-1 crystallized using 1<sup>#</sup>; M-NCM-2 crystallized using 2<sup>#</sup>)

However, the design of the equipments and the process are considerable difficult. HU et al [41] reported that the spherical  $\text{LiNi}_{1/3}\text{Co}_{1/3}\text{Mn}_{1/3}\text{O}_2$  can be prepared based on the co-precipitation method followed by spray drying processes using a stoichiometric amount of spherical spinel  $(\text{CoNiMn})\text{O}_4$  powders and  $\text{LiOH}$ . The initial discharge specific capacities were 189.8 mA·h/g at 0.1C and 167.6 mA·h/g at 1.0C in the voltage range of 3.0–4.5 V; the capacity retention ratios were 93.1% and 62.8% after 50 cycles, respectively.

JU and KANG [42] reported that the Ni–Co–Mn–O precursor powders with spherical shape and dense structures could be obtained from a spray solution, where  $\text{LiNi}_{1/3}\text{Co}_{1/3}\text{Mn}_{1/3}\text{O}_2$  cathode powders with a spherical shape and fine size were formed by solid-state reaction using lithium hydroxide. The mean size of the spherical cathode powders was reported to be 1.1  $\mu\text{m}$ . The discharge capacities of the  $\text{LiNi}_{1/3}\text{Co}_{1/3}\text{Mn}_{1/3}\text{O}_2$  powders were 195 mA·h/g at 0.1C and 183 mA·h/g at 0.5C, and the latter exhibited an 84% capacity retention ratio after 30 cycles.

LIN et al [43] reported the synthesis of porous and spherical  $\text{LiNi}_{1/3}\text{Co}_{1/3}\text{Mn}_{1/3}\text{O}_2$  powders with small particle sizes and good particle size distribution by a slurry spray drying process and calcining at 950 °C. The particles with size of about 40  $\mu\text{m}$  were uniform. They had an initial discharge capacity of 188.9 mA·h/g at 0.2C (32 mA·h/g) and retained 91.4% of the initial discharge capacity from 0.2C to 4.0C rate attributed to the particular morphology.

YUE et al [44] reported that submicron  $\text{LiNi}_{0.6}\text{Co}_{0.2}\text{Mn}_{0.2}\text{O}_2$  can be prepared by a spray drying assisted solid-state method, which had a near-spherical shape with the average particle sizes of about 400 nm to 1  $\mu\text{m}$ . Its lattice parameters  $a$  and  $c$  were similar to the values reported previously. The single-phase layered  $\text{LiNi}_{0.6}\text{Co}_{0.2}\text{Mn}_{0.2}\text{O}_2$  exhibited a reversible charge/

discharge capacity of 179.8 mA·h/g at 0.1C in the voltage range of 2.8–4.3 V. The capacity retention upon cycling was 93.7% at 1.0C after the 40th discharge.

### 3.6 Micro-emulsion method

The micro-emulsion approach is a soft chemical route, which possesses a great potential for synthesizing cathode materials with multiple cations. For example, LU and LIN [45] successfully synthesized  $\text{LiNi}_{1/3}\text{Co}_{1/3}\text{Mn}_{1/3}\text{O}_2$  using lithium nitrate, nickel nitrate, cobalt nitrate and manganese nitrate as the starting materials via a reverse microemulsion route. The sizes of well-crystallized powders were around 45 nm with calcination at 800 °C for 3 h. Within the voltage range of 2.5–4.5 V, the initial discharge capacities of  $\text{LiNi}_{1/3}\text{Co}_{1/3}\text{Mn}_{1/3}\text{O}_2$  at room temperature and 55 °C were 187.2 mA·h/g and 198.4 mA·h/g, respectively. The prepared powders exhibited low irreversible capacity (5.6% at room temperature and 4.4 % at 55 °C) and good capacity retention, exhibiting better rate capability than the solid-state synthesis approach because of the reduced particle size and increased surface area.

### 3.7 Pechini method

The Pechini method is often used to obtain mono- and multi-component oxide materials owing to its good control of the stoichiometry of obtained compounds, but the synthesis process is limited to solutions in which sparingly soluble salts do not undergo precipitation. LIU et al [46] prepared the layered  $\text{LiNi}_{1/3}\text{Co}_{1/3}\text{Mn}_{1/3}\text{O}_2$  by calcining at 900 °C for 10 h with a modified Pechini method. The surfactants used to disperse cations and certain amounts of concentrated nitric acid led to the formation of foamed gel particles. The sample had uniform particle sizes in the range of 100 to 300 nm and little agglomerates; the materials exhibited an initial discharge capacity of 163.8 mA·h/g in the range of 2.8–4.4 V at 0.1C and exhibited improved rate capability performance due to its uniform nanoparticles.

### 3.8 RAPET method

The RAPET (reactions under autogenic pressure at elevated temperature) method is a new method for the synthesis of nano-sized and core-shell nanostructures in the mass production. It is easy to collect the product and requires no further processing. MAHESH et al [47] synthesized  $\text{LiNi}_{1/3}\text{Co}_{1/3}\text{Mn}_{1/3}\text{O}_2$  cathode materials with particle sizes less than 100 nm via RAPET method. A typical cell employing  $\text{LiNi}_{1/3}\text{Co}_{1/3}\text{Mn}_{1/3}\text{O}_2$  as cathode and  $\text{LiTi}_2(\text{PO}_4)_3$  as anode in 5 mol/L  $\text{LiNO}_3$  solution delivers an average output voltage of 1.0 V with a specific capacity of 84 mA·h/g.

## 4 Modification research

The electrochemical performance of batteries is very sensitive to the particle shape and size of  $\text{LiNi}_x\text{Co}_y\text{Mn}_z\text{O}_2$ . Due to the shorter  $\text{Li}^+$  diffusion distances, nano-particulate cathodes are known to exhibit superior rate capabilities and enhanced structural stability, so the micro/nano structured  $\text{LiNi}_x\text{Co}_y\text{Mn}_z\text{O}_2$  has become the research focus. However, the negative effects of nano-crystalline cathodes are prone to form bigger agglomerates during electrode fabrication and react with liquid electrolytes to form various reaction products owing to their very large surface area. Many investigations reported that the doping and surface-coating are useful and effective approaches to improve the electrochemical properties. It is well-known that the doping can improve the stability of electrode by rising the electronic conductivity and deflating polarization, and surface modification can physically isolate or reduce the contact area and limit the dissolution of the cathode in the electrolyte. In this review, the effect of doping and surface modification to micro/nano structured  $\text{LiNi}_x\text{Co}_y\text{Mn}_z\text{O}_2$  is discussed in the following.

### 4.1 Doping

Partial substitution of the  $\text{LiNi}_x\text{Co}_y\text{Mn}_z\text{O}_2$  is an effective approach to improve the conductivity and electrochemical performance. However, the substituents are usually electrochemically inactive elements for electrochemically active elements such as Li, Al, Mg, Fe, F and so on in Li, Ni, Co, Mn or O sites. HONG et al [48] reported that the spherical  $\text{LiNi}_{1/3}\text{Co}_{1/3}\text{Mn}_{1/3}\text{O}_2$  powders with a thin uniform layer of  $[\text{B},\text{Al}]_2\text{O}_3$  on the surface can be obtained via a co-precipitation method. The surface-coated  $\text{LiNi}_{1/3}\text{Co}_{1/3}\text{Mn}_{1/3}\text{O}_2$  particle size was increased by about 1  $\mu\text{m}$  from 10 to 15  $\mu\text{m}$  of the bare  $\text{LiNi}_{1/3}\text{Co}_{1/3}\text{Mn}_{1/3}\text{O}_2$ , in which the thickness of coated layer was about 0.7  $\mu\text{m}$  and the calculated lattice parameter  $c$  was 14.242 and 14.260 Å for the bare and the coated  $\text{LiNi}_{1/3}\text{Co}_{1/3}\text{Mn}_{1/3}\text{O}_2$ , respectively. There was no significant difference in initial discharge capacity. The surface-coated  $\text{LiNi}_{1/3}\text{Co}_{1/3}\text{Mn}_{1/3}\text{O}_2$  showed the discharge capacities of 182 mA·h/g and 177 mA·h/g at 0.1C and 0.2C in the voltage range of 3.0–4.5 V, compared with the bare sample of 181 and 177 mA·h/g, respectively. The capacity retention rate of coated  $\text{LiNi}_{1/3}\text{Co}_{1/3}\text{Mn}_{1/3}\text{O}_2$  after 40 cycles at 1.0C rate maintained 93% of the initial discharge capacity while the rate of bare  $\text{LiNi}_{1/3}\text{Co}_{1/3}\text{Mn}_{1/3}\text{O}_2$  only 88%. The reason for enhancement of retention capacity was attributed to the improvement in the charge transfer kinetics and the stability in electrolyte due to

[B,Al]<sub>2</sub>O<sub>3</sub> coating.

LIAO et al [49] synthesized LiNi<sub>0.6-x</sub>Mg<sub>x</sub>Co<sub>0.25</sub>Mn<sub>0.15</sub>O<sub>2</sub> ( $x=0$  and 0.03) via the mixing hydroxide method. These materials exhibited  $\alpha$ -NaFeO<sub>2</sub> structure as indicated by the XRD patterns. The LiNi<sub>0.57</sub>Mg<sub>0.03</sub>Co<sub>0.25</sub>Mn<sub>0.15</sub>O<sub>2</sub> had the capacity retention of 95% after 20 cycles in the voltage range of 3–4.5 V, which were higher than that of 79% in LiNi<sub>0.6</sub>Co<sub>0.25</sub>Mn<sub>0.15</sub>O<sub>2</sub> and the thermal stability was improved by Mg substitution at every delithiated state of electrodes with electrolytes. The improvements of both electrochemical retention and thermal stability in Mg-doped samples were possibly attributed to the reduced cation mixing and complete structural changes.

LI et al [50] reported that single phase LiNi<sub>0.79</sub>Co<sub>0.1</sub>Mn<sub>0.1</sub>Cr<sub>0.1</sub>O<sub>2</sub> can be synthesized via a fast co-precipitation and anneal method, which exhibited a uniform near-spherical microstructure in the range of 100–500 nm. The discharge capacity of LiNi<sub>0.79</sub>Co<sub>0.1</sub>Mn<sub>0.1</sub>Cr<sub>0.1</sub>O<sub>2</sub> was 209.9 mA·h/g at 0.1C between 2.7 and 4.3 V, with the capacity retention of 89.0% after 50 cycles (Fig. 5). The improved discharge capacity, enhanced rate ability and cycling property resulting from the suitable Cr substitution could suppress the cation mixing and reduced surface concentration of Ni ions. It

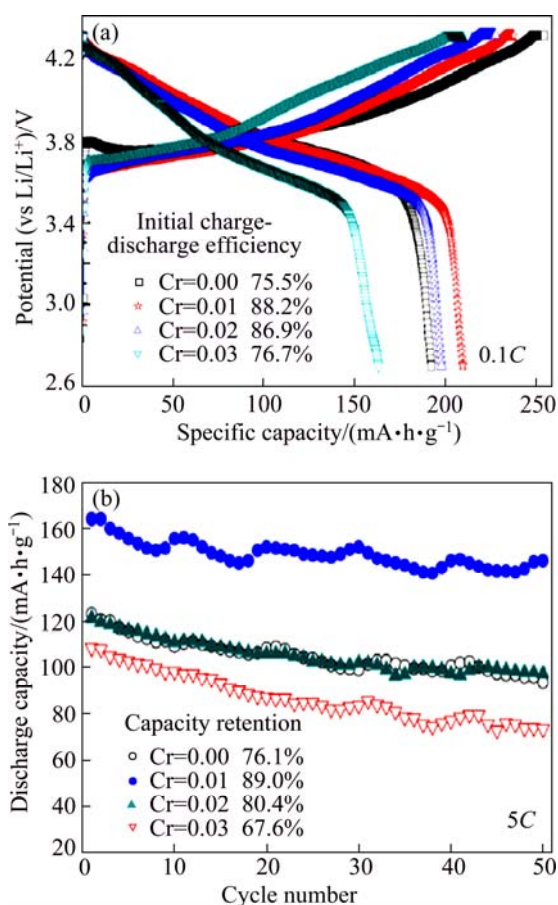


**Fig. 5** Initial charge-discharge curves (a) and cyclic ability (b) of LiNi<sub>0.8-x</sub>Co<sub>0.1</sub>Mn<sub>0.1</sub>Cr<sub>x</sub>O<sub>2</sub> ( $x=0.01, 0.02$  and 0.03) samples

was suggested that excessive Cr substitution might induce partial occupation of Cr<sup>6+</sup> and Mn<sup>3+</sup> in Li layers.

DING et al [51] prepared a series of cathode materials for lithium-ion batteries with the formula Li[Ni<sub>1/3</sub>Co<sub>1/3</sub>Mn<sub>1/3</sub>]<sub>0.97</sub>Re<sub>0.03</sub>O<sub>2</sub> (Re=La, Ce, Pr) by a sol-gel method using citric acid as chelating agent. The initial discharge capacity of all the doped samples was more than 160 mAh/g at a constant current density of 1.0C between 2.6 V and 4.4 V (vs Li) at room temperature (Fig. 6). After 20th cycling, they exhibited about 97% of the initial capacity for the rare earth elements doped samples. The improved discharge capacity resulted from the effect of rare earth elements doping, which was the increase of lattice parameters  $a$  and  $c$  leading to more Li<sup>+</sup> can be extracted/inserted from the active materials. Furthermore, the excellent cycling performance can be contributed to the suppression of increase of charge-transfer resistance during cycling.

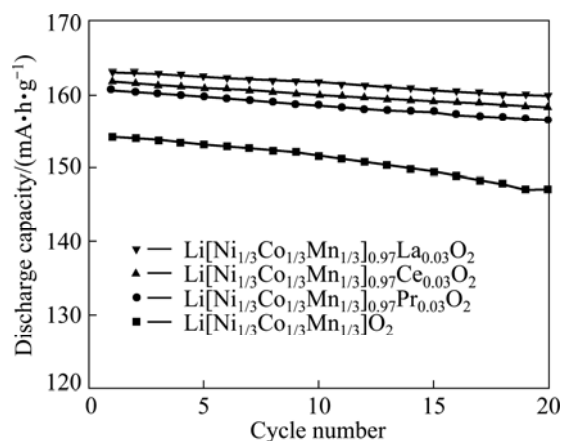


**Fig. 6** Cycling performances of pure LiNi<sub>1/3</sub>Co<sub>1/3</sub>Mn<sub>1/3</sub>O<sub>2</sub> and LiNi<sub>1/3</sub>Co<sub>1/3</sub>Mn<sub>1/3</sub>O<sub>2</sub> with rare earth elements doping

DING et al [52] prepared the LiNi<sub>1/3</sub>Co<sub>1/3</sub>Mn<sub>1/3-x</sub>Al<sub>x</sub>O<sub>2</sub> ( $0 \leq x \leq 0.08$ ) nanofibers by electrospun method using PVP/metal nitrates composites as precursors. The uniform layered structural LiNi<sub>1/3</sub>Co<sub>1/3</sub>Mn<sub>1/3-x</sub>Al<sub>x</sub>O<sub>2</sub> nanofibers have an average diameter of less than 100 nm. The initial discharge capacity of LiNi<sub>1/3</sub>Co<sub>1/3</sub>Mn<sub>1/3-0.06</sub>Al<sub>0.06</sub>O<sub>2</sub> nanofibers was 186.59 mA·h/g in the range of 3.0–4.3 V at 0.1C. After 30 cycles, the capacity retention reached 96.11% (Fig. 7). They suggested that a reasonable amount introduction of aluminum content brought increasing content of transition metal ions with low valence and resulted in expansion in the lattice volume, while superfluous Al<sup>3+</sup> caused the structural instability and deteriorated the electrochemical performance renewal.

WANG et al [53] prepared LiNi<sub>0.305</sub>Mn<sub>0.33</sub>Co<sub>0.33</sub>Y<sub>0.025</sub>O<sub>2</sub> by Y<sup>3+</sup> substitution of Ni<sup>2+</sup> using sol-gel method. The XRD analysis showed that the lattice parameter  $c$  became larger, the LiNi<sub>0.305</sub>Mn<sub>0.33</sub>Co<sub>0.33</sub>Y<sub>0.025</sub>O<sub>2</sub> had

capacity retention of 95.9% after 40 cycles at 4.0C, which was related to the larger lattice parameter caused by Y doping, enabling  $\text{Li}^+$  ions diffusion in the layered oxide compound. The reason for higher capacity retention and superior rate capability of Y-doped samples can be ascribed to restraining the increase of charge transfer resistance of cathode during cycling.

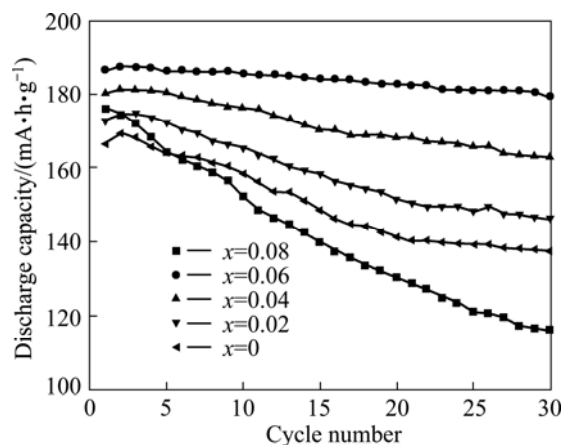


**Fig. 7** Capacity retention of  $\text{LiNi}_{1/3}\text{Co}_{1/3}\text{Mn}_{1/3-x}\text{Al}_x\text{O}_2$  nanofibers

#### 4.2 Surface modification

The materials which are used as surface modifiers include metals, metal oxides and inorganic salts. Compared with lattice doping, coatings and composites were proven to enhance effectively the performance of micro/nano structured  $\text{LiNi}_x\text{Co}_y\text{Mn}_z\text{O}_2$ , and the structural stabilization, good cycle ability, and thermal stability even at a highly oxidized state are attributed to the suppression of phase transitions associated with the intercalation–deintercalation processes by high-fracture-tough coating materials.

VENKATESWARA et al [54] reported that  $\text{LiNi}_{1/3}\text{Co}_{1/3}\text{Mn}_{1/3}\text{O}_2$  and  $\text{LiNi}_{1/3}\text{Co}_{1/3}\text{Mn}_{1/3}\text{O}_2$ -graphene composite (90%:10%) with the average particle size of 70–110 nm could be prepared by microemulsion and ball-milling techniques, respectively. The calculated lattice constants ( $a=2.851 \text{ \AA}$  and  $c=14.219 \text{ \AA}$ ) are in good agreement with the literature values. It exhibited higher discharge capacities at different current rates and also less irreversible capacity losses when compared with  $\text{LiNi}_{1/3}\text{Co}_{1/3}\text{Mn}_{1/3}\text{O}_2$ , which was attributed to an increase in the grain connectivity and high electronic conductivity.

SONG et al [55] reported that a  $\text{Li}[\text{Ni}_{0.4}\text{Co}_{0.3}\text{Mn}_{0.3}]\text{O}_2$  cathode was modified by applying a  $\text{La}_{2/3-x}\text{Li}_{3x}\text{TiO}_3$  (LLT) coating, the surface of coated sample was rough and had nanoparticles attached. The rate capability was effectively improved when the sample was coated with a material having high La and

low Li content. On the contrary, the discharge capacity under a high cut-off voltage was greatly enhanced, which is attributed to the coating layer which acts as an effective lithium-ion conductor and also functions as a protective layer against attack from the electrolyte. Overall, the thermal stability of the  $\text{Li}[\text{Ni}_{0.4}\text{Co}_{0.3}\text{Mn}_{0.3}]\text{O}_2$  electrode was improved by coating LLT, due to the suppression of the dissolution of transition metals during storage at a high temperature.

SONG et al [56] reported that  $\text{LaF}_3$  and  $\text{MgF}_2$  were introduced for the surface modification of an  $\text{Li}[\text{Ni}_{0.5}\text{Co}_{0.2}\text{Mn}_{0.3}]\text{O}_2$  electrode. The authors found that these tough materials maintained a relatively higher discharge capacity than the pristine sample at high C rates (Fig. 8), while the  $\text{MgF}_2$ -coated electrode provided a more advanced cyclic performance in the high voltage range than the  $\text{LaF}_3$ -coated electrode, and  $\text{MgF}_2$ -coated electrode significantly enhanced the thermal stability according to DSC analysis.

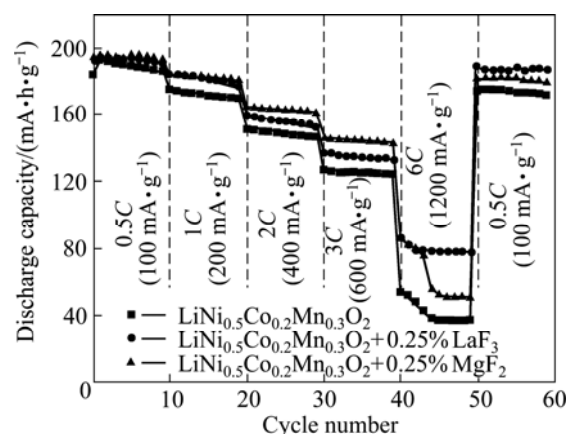


**Fig. 8** Discharge capacities and cyclic performances of pristine and coated  $\text{Li}[\text{Ni}_{0.5}\text{Co}_{0.2}\text{Mn}_{0.3}]\text{O}_2$  electrodes in voltage range of 4.6–3.0 V at rates of 0.5C, 1C, 2C, 3C, and 6C

GHANTY et al [57] systematically studied the electrochemical characteristics of  $x\text{Li}_2\text{MnO}_3-(1-x)\text{Li}(\text{Mn}_{0.375}\text{Ni}_{0.375}\text{Co}_{0.25})\text{O}_2$  ( $0 \leq x \leq 1.0$ ) integrated cathode materials prepared by auto-combustion synthesis route. For  $x=0.5$ , the powders  $0.5\text{Li}_2\text{MnO}_3-0.5\text{Li}(\text{Mn}_{0.375}\text{Ni}_{0.375}\text{Co}_{0.25})\text{O}_2$  cathode have discharge capacity of 290  $\text{mA}\cdot\text{h}/\text{g}$  with capacity retention of 220  $\text{mA}\cdot\text{h}/\text{g}$  at 10  $\text{mA}/\text{g}$  in the voltage range between 2.5 to 4.8 V after 50 cycles, and this composition also exhibits energy density of 1018 and 747  $\text{mW}\cdot\text{h}/\text{g}$  at the 1st and 50th cycle, respectively. While  $0.75\text{Li}_2\text{MnO}_3-0.25\text{Li}(\text{Mn}_{0.375}\text{Ni}_{0.375}\text{Co}_{0.25})\text{O}_2$  cathode exhibited a discharge capacity of 235  $\text{mA}\cdot\text{h}/\text{g}$  and excellent capacity retention up to 50 cycles. The better rate capability is attributed to its finer particle size, which makes diffusion distance of lithium ion intercalation shorter, and the high energy density of lithium batteries is mainly due to the

reversible spinel transformation and  $\text{Mn}^{3+}/\text{Mn}^{4+}$  redox couple (below 3.0 V regime).

LEE et al [58] synthesized micro-scale cor-shell spherical structured powders  $\text{Li}[(\text{Ni}_{1/3}\text{Co}_{1/3}\text{Mn}_{1/3})_{0.8}(\text{Ni}_{1/2}\text{Mn}_{1/2})_{0.2}]\text{O}_2$  via a co-precipitation method. The core-shell particle consists of  $\text{Li}[\text{Ni}_{1/3}\text{Co}_{1/3}\text{Mn}_{1/3}]\text{O}_2$  with the particle diameter of 8  $\mu\text{m}$  as the core and  $\text{LiNi}_{1/2}\text{Mn}_{1/2}\text{O}_2$  with the particle diameter of 1  $\mu\text{m}$  as the shell. The initial charge–discharge capacities showed 180.5  $\text{mA}\cdot\text{h}/\text{g}$  of the core, 177.0  $\text{mA}\cdot\text{h}/\text{g}$  of the core-shell, and 156.2  $\text{mA}\cdot\text{h}/\text{g}$  of the shell, respectively between 3.0 and 4.5 V versus Li at a constant current density of 100  $\text{mA}/\text{g}$ . In comparison, the core-shell structured  $\text{Li}[(\text{Ni}_{1/3}\text{Co}_{1/3}\text{Mn}_{1/3})_{0.8}(\text{Ni}_{1/2}\text{Mn}_{1/2})_{0.2}]\text{O}_2$  cell exhibited excellent capacity retention of 98.8% at 30 °C during 100 cycles, because the core material was buffered by the encapsulation by the shell of  $\text{Li}[\text{Ni}_{0.5}\text{Mn}_{0.5}]\text{O}_2$ . It had a significant improvement in the high-voltage cycling performance, which was probably due to the  $\text{Li}[\text{Ni}_{0.5}\text{Mn}_{0.5}]\text{O}_2$  shell protecting the structural deformation of the core  $\text{Li}[\text{Ni}_{1/3}\text{Co}_{1/3}\text{Mn}_{1/3}]\text{O}_2$  material at high voltage. Furthermore, the core-shell material had exothermic onset temperature of approximately 272 °C, which was higher than that of the core material of 261 °C in the highly delithiated state. The reason for thermal stability was the absence of tetravalent Co and the presence of tetravalent Mn in the shell, meanwhile, Ni valence did not completely reach the tetravalent state.

GU and JIAN [59] fabricated hollow  $\text{LiNi}_{0.8}\text{Co}_{0.1}\text{Mn}_{0.1}\text{O}_2\text{-MgO}$  core-shell fibers for the first time by coaxial electrospinning combined with the sol–gel method, in which process, the formation of hollow structure was attributed to the polyvinyl pyrrolidone (PVP). The hollow  $\text{LiNi}_{0.8}\text{Co}_{0.1}\text{Mn}_{0.1}\text{O}_2\text{-MgO}$  coaxial fibers had an outer diameter of 1–2  $\mu\text{m}$ , but the shell thickness of the hollow coaxial fibers was 30–60 nm and the wall thickness was 300–500 nm. The hollow  $\text{LiNi}_{0.8}\text{Co}_{0.1}\text{Mn}_{0.1}\text{O}_2\text{-MgO}$  core-shell fiber electrode had a higher initial charge-discharge capacity of 195  $\text{mA}\cdot\text{h}/\text{g}$  than those of 184  $\text{mA}\cdot\text{h}/\text{g}$  of solid fibers at a constant current density of 20  $\text{mA}/\text{g}$  in the voltage range from 3.0 to 4.3 V, corresponded to 89.2% and 86.4% of the capacity retention rate after 50 cycles, respectively. Except for the structure-stabilizing effect of the MgO coating, the superior electrochemical performance might result from the relatively high specific surface area of the hollow tubular structure and faster kinetics, which offer more active positions for lithium ion intercalating/deintercalating and reduce the  $\text{Li}^+$  intercalation rate density per unit area.

SUN et al [60] synthesized a high-energy functional cathode material with an average composition of

$\text{Li}[\text{Ni}_{0.72}\text{Co}_{0.18}\text{Mn}_{0.10}]\text{O}_2$  via a co-precipitation method, which was composed of a core of about 6  $\mu\text{m}$  thickness  $\text{Li}[\text{Ni}_{0.8}\text{Co}_{0.2}]\text{O}_2$  and a concentration-gradient shell with an approximately 1  $\mu\text{m}$  outer shell with composition of  $\text{Li}[\text{Ni}_{0.55}\text{Co}_{0.15}\text{Mn}_{0.30}]\text{O}_2$ . It had excellent cyclability with a capacity retention of 95.3% between 3.0 and 4.3 V at a current rate of 40  $\text{mA}/\text{g}$  (0.2C-rate) after 50 cycles, while the  $\text{Li}[\text{Ni}_{0.8}\text{Co}_{0.2}]\text{O}_2$  core exhibited a capacity retention of only 66%. Its electrochemical and thermal properties were superior to those of the core  $\text{Li}[\text{Ni}_{0.8}\text{Co}_{0.2}]\text{O}_2$  material alone. The reason for improvements is a gradual and continuous increase of the stable tetravalent Mn in the concentration-gradient shell layer. The powders had a well-defined layer structure based on a hexagonal  $\alpha\text{-NaFeO}_2$  structure, and TEM showed that the structural integrity remained intact during cycling.

## 5 Conclusion and perspective

The electrochemical properties of  $\text{LiNi}_x\text{Co}_y\text{Mn}_z\text{O}_2$  electrode materials strongly depend on the particle size, morphology, stoichiometric proportion and homogeneity. However, the particle size has greater influence on the improved performances [61]. Due to the synergistic effect of three transition-metal element ions and many possible compositional options, these multi-component oxides are expected to inherit the merits of each component material and might even prevail in the overall performance. Thus, the dependence of cathode performance on the composition of  $\text{LiNi}_x\text{Co}_y\text{Mn}_z\text{O}_2$  is crucial for the practical applications of these multi-component transition-metal element oxide materials. Enhanced performances of  $\text{LiNi}_x\text{Co}_y\text{Mn}_z\text{O}_2$  electrode materials such as higher capacity, improved rate capability, and sustained capacity retention for longer cycles, were achieved by various nanostructures with doping and coating. It is imperative that various hybrid nanostructures will represent one of the most attractive strategies to surpass the limitations associated with single phase nanomaterials [62,63]. The combination of novel synthetic method with strategic design of their shape on the nanometer scale and novel nanoscience and nanotechnology will enable a breakthrough to overcome these problems experienced by present technologies [64]. It is clear that numerous efforts in advanced electrode materials, electrode structure design and device fabrication [65] will be quickly proved fruitful in the near future.

## References

- [1] CENTI G, PERATHONER S. The role of nanostructure in

- improving the performance of electrodes for energy storage and conversion [J]. *European Journal of Inorganic Chemistry*, 2009, 2009(26): 3851–3878.
- [2] BAZITO F F C, TORRESI R M. Cathodes for lithium ion batteries: The benefits of using nanostructured materials [J]. *Journal of the Brazilian Chemical Society*, 2006, 17(4): 627–642.
- [3] SONG M K, PARK S, ALAMGIR F M, CHO J, LIU M L. Nanostructured electrodes for lithium-ion and lithium-air batteries: The latest developments, challenges, and perspectives [J]. *Materials Science and Engineering R: Reports*, 2011, 72(11): 203–252.
- [4] KIM M G, CHO J. Reversible and high-capacity nanostructured electrode materials for Li-ion batteries [J]. *Advanced Functional Materials*, 2009, 19(10): 1497–1514.
- [5] JI Li-wen, LIN Zhan, ALCOUTLABI M, ZHANG Xiang-wu. Recent developments in nanostructured anode materials for rechargeable lithium-ion batteries [J]. *Energy Environ Sci*, 2011, 4(8): 2682–2699.
- [6] DIMESSO L, FÖRSTER C, JAEGERMANN W, KHANDERI J P, TEMPEL H, POPP A, ENGSTLER J, SCHNEIDER J J, SARAPULOVA A, MIKHAILOVA D. Developments in nanostructured  $\text{LiMPO}_4$  (M=Fe, Co, Ni, Mn) composites based on three dimensional carbon architecture [J]. *Chemical Society Reviews*, 2012, 41: 5068–5080.
- [7] HE Ping, YU Hai-jun, ZHOU Hao-shen. Layered lithium transition metal oxide cathodes towards high energy lithium-ion batteries [J]. *J Mater Chem*, 2012, 22(9): 3680–3695.
- [8] LIU Z L, YU A, LEE J Y. Synthesis and characterization of  $\text{LiNi}_{1-x-y}\text{Co}_x\text{Mn}_y\text{O}_2$  as the cathode materials of secondary lithium batteries [J]. *Journal of Power Sources*, 1999, 81–82: 416–419.
- [9] LEE S, PARK S S. Atomistic simulation study of mixed-metal oxide ( $\text{LiNi}_{1/3}\text{Co}_{1/3}\text{Mn}_{1/3}\text{O}_2$ ) cathode material for lithium ion battery [J]. *The Journal of Physical Chemistry C*, 2012, 116(10): 6484–6489.
- [10] WANG Li, LI Jian-gang, HE Xiang-ming, PU Wei-hua, WAN Chun-rong, JIANG Chang-yin. Recent advances in layered  $\text{LiNi}_x\text{Co}_y\text{Mn}_{1-x-y}\text{O}_2$  cathode materials for lithium ion batteries [J]. *Journal of Solid State Electrochemistry*, 2009, 13(8): 1157–1164.
- [11] CHERNOVA N A, MA M, XIAO J, WHITTINGHAM M S, BREGER J, GREY C P. Layered  $\text{Li}_x\text{Ni}_y\text{Mn}_z\text{Co}_{(1-2x)}\text{O}_2$  cathodes for lithium ion batteries: Understanding local structure via magnetic properties [J]. *Chemistry of Materials*, 2007, 19(19): 4682–4693.
- [12] IGAWA N, TAGUCHI T, FUKAZAWA H, YAMAUCHI H, UTSUMI W. Crystal structure and nuclear density distribution of  $\text{LiCo}_{1/3}\text{Ni}_{1/3}\text{Mn}_{1/3}\text{O}_2$  analyzed by Rietveld/maximum entropy method [J]. *Journal of the American Ceramic Society*, 2010, 93(8): 2144–2146.
- [13] ZENG D L, CABANA J, BRÉGER J, YOON W S, GREY C P. Cation ordering in  $\text{Li}[\text{Ni}_x\text{Mn}_x\text{Co}_{(1-2x)}]\text{O}_2$ -layered cathode materials: A nuclear magnetic resonance (NMR), pair distribution function, X-ray absorption spectroscopy, and electrochemical study [J]. *Chemistry of Materials*, 2007, 19(25): 6277–6289.
- [14] BIE X F, LIU L N, EHRENBERG H, WEI Y J, NIKOLOWSKI K, WANG C Z, UEDA Y, CHEN G, CHEN H, DU F. Revisit on the layered  $\text{LiNi}_{0.4}\text{Mn}_{0.4}\text{Co}_{0.2}\text{O}_2$ : A magnetic approach [J]. *RSC Advances*, 2012, 2(26): 9986–9992.
- [15] YABUUCHI N, YOSHII K, MYUNG S T, NAKAI I, KOMABA S. Detailed studies of a high-capacity electrode material for rechargeable batteries,  $\text{Li}_2\text{MnO}_3$ - $\text{LiCo}_{1/3}\text{Ni}_{1/3}\text{Mn}_{1/3}\text{O}_2$  [J]. *Journal of the American Chemical Society*, 2011, 133(12): 4404–4419.
- [16] MAHESH K C, MANJUNATHA H, VENKATESHA T V, SURESH G S. Study of lithium ion intercalation/de-intercalation into  $\text{LiNi}_{1/3}\text{Mn}_{1/3}\text{Co}_{1/3}\text{O}_2$  in aqueous solution using electrochemical impedance spectroscopy [J]. *Journal of Solid State Electrochemistry*, 2012, 16(9): 3011–3025.
- [17] NGALA J K, CHERNOVA N A, MA M M, MAMAK M, ZAVALIU P Y, WHITTINGHAM M S. The synthesis, characterization and electrochemical behavior of the layered  $\text{LiNi}_{0.4}\text{Mn}_{0.4}\text{Co}_{0.2}\text{O}_2$  compound [J]. *J Mater Chem*, 2004, 14(2): 214–220.
- [18] PARK B C, BANG H J, YOON C S, MYUNG S T, PRAKASH J, SUN Y K. Structural transformation of  $\text{Li}[\text{Ni}_{0.5-x}\text{Co}_{2x}\text{Mn}_{0.5-x}]\text{O}_2$  ( $2x \leq 0.1$ ) charged in high-voltage range (4.5 V) [J]. *Journal of the Electrochemical Society A*, 2007, 154(6): 520–526.
- [19] JEON Y A, KIM S K, KIM Y S, WON D H, KIM B I, NO K S. A first principles investigation of new cathode materials for advanced lithium batteries [J]. *Journal of Electroceramics*, 2006, 17(2): 667–671.
- [20] TSAI Y W, LEE J F, LIU D G, HWANG B J. In-situ X-ray absorption spectroscopy investigations of a layered  $\text{LiNi}_{0.65}\text{Co}_{0.25}\text{Mn}_{0.1}\text{O}_2$  cathode material for rechargeable lithium batteries [J]. *J Mater Chem*, 2004, 14(6): 958–965.
- [21] LUO Gai-xia, ZHAO Ji-jun, KE Xue-zhi, ZHANG Peng-bo, SUN Hou-qian, WANG Bao-lin. Structure, electrode voltage and activation energy of  $\text{LiMn}_x\text{Co}_y\text{Ni}_{1-x-y}\text{O}_2$  solid solutions as cathode materials for Li batteries from first-principles [J]. *Journal of the Electrochemical Society A*, 2012, 159(8): 1203–1208.
- [22] WANG Lei, LI Jian-gang, CHI Na, YU Hai-ying, DONG Tao. Comparison of electrochemical performance of  $\text{LiNi}_{0.7}\text{Co}_{0.15}\text{Mn}_{0.15}\text{O}_2$  with different surface composition [J]. *Advanced Materials Research*, 2012, 554–556: 445–449.
- [23] KIM J M, CHUNG H T. Role of transition metals in layered  $\text{Li}[\text{Ni},\text{Co},\text{Mn}]\text{O}_2$  under electrochemical operation [J]. *Electrochimica Acta*, 2004, 49(21): 3573–3580.
- [24] SUN Y K, KANG H B, MYUNG S T, PRAKASH J. Effect of manganese content on the electrochemical and thermal stabilities of  $\text{Li}[\text{Ni}_{0.58}\text{Co}_{0.28-x}\text{Mn}_{0.14+x}]\text{O}_2$  cathode materials for lithium-ion batteries [J]. *Journal of the Electrochemical Society A*, 2010, 157(12): 1335–1340.
- [25] DAHBI M, SAADOUNE I, GUSTAFSSON T, EDSTRÖM K. Effect of manganese on the structural and thermal stability of  $\text{Li}_{0.3}\text{Ni}_{0.7-y}\text{Co}_{0.3-y}\text{Mn}_y\text{O}_2$  electrode materials ( $y=0$  and  $0.05$ ) [J]. *Solid State Ionics*, 2011, 203(1): 37–41.
- [26] GU Yi-jie, CHEN Yun-bo, LIU Hong-quan, WANG Yan-ming, WANG Cui-ling, WU Hui-kang. Structural characterization of layered  $\text{LiNi}_{0.85-x}\text{Mn}_x\text{Co}_{0.15}\text{O}_2$  with  $x=0, 0.1, 0.2$  and  $0.4$  oxide electrodes for Li batteries [J]. *Journal of Alloys and Compounds*, 2011, 509(30): 7915–7921.
- [27] WANG Jun, ZHANG Ming-hao, TANG Chang-lin, XIA Yong-gao, LIU Zhao-ping. Microwave-irradiation synthesis of  $\text{Li}_{1/3}\text{Ni}_x\text{Co}_y\text{Mn}_{1-x-y}\text{O}_{2.4}$  cathode materials for lithium ion batteries [J]. *Electrochimica Acta*, 2012, 80: 15–21.
- [28] OHZUKU T, MAKIMURA Y. Layered lithium insertion material of  $\text{LiCo}_{1/3}\text{Ni}_{1/3}\text{Mn}_{1/3}\text{O}_2$  for lithium-ion batteries [J]. *Chemistry Letters*, 2001, 30(7): 642–643.
- [29] TAN Long, LIU Hao-wen. High rate charge-discharge properties of  $\text{LiNi}_{1/3}\text{Co}_{1/3}\text{Mn}_{1/3}\text{O}_2$  synthesized via a low temperature solid-state method [J]. *Solid State Ionics*, 2010, 181(33–34): 1530–1533.
- [30] DOU Shu-mei, WANG Wen-lou. Synthesis and electrochemical properties of layered  $\text{LiNi}_{0.5-x}\text{Mn}_{0.5-x}\text{Co}_{2x}\text{O}_2$  for lithium-ion battery from nickel manganese cobalt oxide precursor [J]. *Journal of Solid State Electrochemistry*, 2011, 15(2): 399–404.

- [31] DENG C, ZHANG S, MA L, SUN Y H, YANG S Y, FU B L, LIU F L, WU Q. Effects of precipitator on the morphological, structural and electrochemical characteristics of Li<sub>1/3</sub>[Ni<sub>1/3</sub>Co<sub>1/3</sub>Mn<sub>1/3</sub>]O<sub>2</sub> prepared via carbonate coprecipitation [J]. *Journal of Alloys and Compounds*, 2011, 509(4): 1322–1327.
- [32] YANG Shun-yi, WANG Xian-you, YANG Xiu-kang, LIU Li, LIU Zi-ling, BAI Yan-song, WANG Ying-ping. Influence of Li source on tap density and high rate cycling performance of spherical Li[Ni<sub>1/3</sub>Co<sub>1/3</sub>Mn<sub>1/3</sub>]O<sub>2</sub> for advanced lithium-ion batteries [J]. *Journal of Solid State Electrochemistry*, 2012, 16(3): 1229–1237.
- [33] HUANG Zhen-lei, GAO Jian, HE Xiang-ming, LI Jian-jun, JIANG Chang-yin. Well-ordered spherical LiNi<sub>x</sub>Co<sub>(1-2x)</sub>Mn<sub>x</sub>O<sub>2</sub> cathode materials synthesized from cobalt concentration-gradient precursors [J]. *Journal of Power Sources*, 2011, 202: 284–290.
- [34] MYUNG S T, LEE M H, KOMABA S, KUMAGAI N, SUN Y K. Hydrothermal synthesis of layered Li[Ni<sub>1/3</sub>Co<sub>1/3</sub>Mn<sub>1/3</sub>]O<sub>2</sub> as positive electrode material for lithium secondary battery [J]. *Electrochimica Acta*, 2005, 50(24): 4800–4806.
- [35] LU C H, SHEN B J. Electrochemical characteristics of LiNi<sub>1/3</sub>Co<sub>1/3</sub>Mn<sub>1/3</sub>O<sub>2</sub> powders prepared from microwave-hydrothermally derived precursors [J]. *Journal of Alloys and Compounds*, 2010, 497(1–2): 159–165.
- [36] XIE Jun-lan, HUANG Xiang, ZHU Zhi-bin, DAI Jin-hui. Hydrothermal synthesis of Li(Ni<sub>1/3</sub>Co<sub>1/3</sub>Mn<sub>1/3</sub>)O<sub>2</sub> for lithium rechargeable batteries [J]. *Ceramics International*, 2010, 36(8): 2485–2487.
- [37] WU Feng, WANG Meng, SU Yue-feng, BAO Li-ying, CHEN Shi. A novel method for synthesis of layered LiNi<sub>1/3</sub>Mn<sub>1/3</sub>Co<sub>1/3</sub>O<sub>2</sub> as cathode material for lithium-ion battery [J]. *Journal of Power Sources*, 2010, 195(8): 2362–2367.
- [38] SHAJU K M, BRUCE P G. Macroporous Li(Ni<sub>1/3</sub>Co<sub>1/3</sub>Mn<sub>1/3</sub>)O<sub>2</sub>: A high-power and high-energy cathode for rechargeable lithium batteries [J]. *Advanced Materials*, 2006, 18(17): 2330–2334.
- [39] HUANG Z D, LIU X M, OH S W, ZHANG B, MA P C, KIM J K. Microscopically porous, interconnected single crystal LiNi<sub>1/3</sub>Co<sub>1/3</sub>Mn<sub>1/3</sub>O<sub>2</sub> cathode material for lithium ion batteries [J]. *J Mater Chem*, 2011, 21(29): 10777–10784.
- [40] NITHYA C, KUMARI V S S, GOPUKUMAR S. Synthesis of high voltage (4.9 V) cycling LiNi<sub>x</sub>Co<sub>y</sub>Mn<sub>1-x-y</sub>O<sub>2</sub> cathode materials for lithium rechargeable batteries [J]. *Physical Chemistry Chemical Physics*, 2011, 13(13): 6125–6132.
- [41] HU S K, CHENG G H, CHENG M Y, HWANG B J, SANTHANAM R. Cycle life improvement of ZrO<sub>2</sub>-coated spherical LiNi<sub>1/3</sub>Co<sub>1/3</sub>Mn<sub>1/3</sub>O<sub>2</sub> cathode material for lithium ion batteries [J]. *Journal of Power Sources*, 2009, 188(2): 564–569.
- [42] JU S H, KANG Y C. The characteristics of Ni–Co–Mn–O precursor and Li(Ni<sub>1/3</sub>Co<sub>1/3</sub>Mn<sub>1/3</sub>)O<sub>2</sub> cathode powders prepared by spray pyrolysis [J]. *Ceramics International*, 2009, 35(3): 1205–1210.
- [43] LIN Bin, WEN Zhao-yin, GU Zhong-hua, HUANG Sha-hua. Morphology and electrochemical performance of Li[Ni<sub>1/3</sub>Co<sub>1/3</sub>Mn<sub>1/3</sub>]O<sub>2</sub> cathode material by a slurry spray drying method [J]. *Journal of Power Sources*, 2008, 175(1): 564–569.
- [44] YUE Peng, WANG Zhi-xing, PENG Wen-jie, LI Ling-jun, GUO Hua-jun, LI Xin-hai, HU Qi-yang, ZHANG Yue-he. Preparation and electrochemical properties of submicron LiNi<sub>0.6</sub>Co<sub>0.2</sub>Mn<sub>0.2</sub>O<sub>2</sub> as cathode material for lithium ion batteries [J]. *Scripta Materialia*, 2011, 65(12): 1077–1080.
- [45] LU C H, LIN Y K. Microemulsion preparation and electrochemical characteristics of LiNi<sub>1/3</sub>Co<sub>1/3</sub>Mn<sub>1/3</sub>O<sub>2</sub> powders [J]. *Journal of Power Sources*, 2009, 189(1): 40–44.
- [46] LIU Xian-ming, GAO Wen-liang, JI Bao-ming. Synthesis of LiNi<sub>1/3</sub>Co<sub>1/3</sub>Mn<sub>1/3</sub>O<sub>2</sub> nanoparticles by modified Pechini method and their enhanced rate capability [J]. *Journal of Sol-Gel Science and Technology*, 2012, 61(1): 56–61.
- [47] MAHESH K C, MANJUNATHA H, SHIVASHANKARAIAH R B, SURESH G S, VENKATESHA T V. Synthesis of LiNi<sub>1/3</sub>Mn<sub>1/3</sub>Co<sub>1/3</sub>O<sub>2</sub> cathode material and its electrochemical characterization in an aqueous electrolyte [J]. *Journal of The Electrochemical Society A*, 2012, 159(7): 1040–1047.
- [48] HONG T E, JEONG E D, BAEK S R, BYEON M R, LEE Y S, KHAN F N, YANG H S. Nano SIMS characterization of boron- and aluminum-coated LiNi<sub>1/3</sub>Co<sub>1/3</sub>Mn<sub>1/3</sub>O<sub>2</sub> cathode materials for lithium secondary ion batteries [J]. *Journal of Applied Electrochemistry*, 2011, 42(1): 41–46.
- [49] LIAO P Y, DUH J G, SHEU H S. Structural and thermal properties of LiNi<sub>0.6-x</sub>Mg<sub>x</sub>Co<sub>0.25</sub>Mn<sub>0.15</sub>O<sub>2</sub> cathode materials [J]. *Journal of Power Sources*, 2008, 183(2): 766–770.
- [50] LI Ling-jun, WANG Zhi-xing, LIU Qi-cheng, YE Chang, CHEN Zhao-yong, GONG Li. Effects of chromium on the structural, surface chemistry and electrochemical of layered LiNi<sub>0.8-x</sub>Co<sub>0.1</sub>Mn<sub>0.1</sub>Cr<sub>x</sub>O<sub>2</sub> [J]. *Electrochimica Acta*, 2012, 77: 89–96.
- [51] DING Yan-huai, ZHANG Ping, JIANG Yong, GAO De-shu. Effect of rare earth elements doping on structure and electrochemical properties of LiNi<sub>1/3</sub>Co<sub>1/3</sub>Mn<sub>1/3</sub>O<sub>2</sub> for lithium-ion battery [J]. *Solid State Ionics*, 2007, 178(13–14): 967–971.
- [52] DING Yan-huai, ZHANG Ping, LONG Zhi-lin, JIANG Yong, XU Fu. Morphology and electrochemical properties of Al doped LiNi<sub>1/3</sub>Co<sub>1/3</sub>Mn<sub>1/3</sub>O<sub>2</sub> nanofibers prepared by electrospinning [J]. *Journal of Alloys and Compounds*, 2009, 487(1): 507–510.
- [53] WANG Meng, CHEN Yun-bo, WU Feng, SU Yue-feng, CHEN Lin, WANG Dong-liang. Characterization of yttrium substituted LiNi<sub>0.33</sub>Mn<sub>0.33</sub>Co<sub>0.33</sub>O<sub>2</sub> cathode material for lithium secondary cells [J]. *Electrochimica Acta*, 2010, 55(28): 8815–8820.
- [54] VENKATESWARA R C, LEELA M R A, ISHIKAWA Y, AJAYAN P M. LiNi<sub>1/3</sub>Co<sub>1/3</sub>Mn<sub>1/3</sub>O<sub>2</sub> graphene composite as a promising cathode for lithium-ion batteries [J]. *ACS Applied Materials & Interfaces*, 2011, 3(8): 2966–2972.
- [55] SONG H G, KIM J Y, PARK Y J. Enhanced electrochemical and storage properties of La<sub>2/3-x</sub>Li<sub>3x</sub>TiO<sub>3</sub>-coated Li[Ni<sub>0.4</sub>Co<sub>0.3</sub>Mn<sub>0.3</sub>]O<sub>2</sub> [J]. *Electrochimica Acta*, 2011, 56(20): 6896–6905.
- [56] SONG H G, KIM S B, PARK Y J. Enhanced electrochemical properties of Li[Ni<sub>0.5</sub>Co<sub>0.2</sub>Mn<sub>0.3</sub>]O<sub>2</sub> cathode by surface coating using LaF<sub>3</sub> and MgF<sub>2</sub> [J]. *Journal of Electroceramics*, 2012, 29(2): 163–169.
- [57] GHANTY C, BASU R N, MAJUMDER S B. Performance of wet chemical synthesized xLi<sub>2</sub>MnO<sub>3</sub>-(1-x)Li(Mn<sub>0.375</sub>Ni<sub>0.375</sub>Co<sub>0.25</sub>)O<sub>2</sub> (0.0 ≤ x ≤ 1.0) integrated cathode for lithium rechargeable battery [J]. *Journal of The Electrochemical Society A*, 2012, 159(7): 1125–1134.
- [58] LEE K S, MYUNG S T, SUN Y K. Synthesis and electrochemical performances of core-shell structured Li[(Ni<sub>1/3</sub>Co<sub>1/3</sub>Mn<sub>1/3</sub>)<sub>0.8</sub>(Ni<sub>1/2</sub>Mn<sub>1/2</sub>)<sub>0.2</sub>]O<sub>2</sub> cathode material for lithium ion batteries [J]. *Journal of Power Sources*, 2010, 195(18): 6043–6048.
- [59] GU Yuan-xiang, JIAN Fang-fang. Hollow LiNi<sub>0.8</sub>Co<sub>0.1</sub>Mn<sub>0.1</sub>O<sub>2</sub>-MgO coaxial fibers: Sol-gel method combined with co-electrospun preparation and electrochemical properties [J]. *The Journal of Physical Chemistry C*, 2008, 112(51): 20176–20180.
- [60] SUN Y K, KIM D H, YOON C S, MYUNG S T, PRAKASH J, AMINE K. A novel cathode material with a concentration-gradient

- for high-energy and safe lithium-ion batteries [J]. *Advanced Functional Materials*, 2010, 20(3): 485–491.
- [61] KIANI M A, MOUSAVI M F, RAHMANIFAR M S. Synthesis of nano and micro-particles of  $\text{LiMn}_2\text{O}_4$ : Electrochemical investigation and assessment as a cathode in Li battery [J]. *Int J Electrochem Sci*, 2011, 6: 2581–2595.
- [62] REDDY A L M, GOWDA S R, SHAIJUMON M M, AJAYAN P M. Hybrid nanostructures for energy storage applications [J]. *Advanced Materials*, 2012, 24(37): 50545–5064.
- [63] LIU R, DUAY J, LEE S B. Heterogeneous nanostructured electrode materials for electrochemical energy storage [J]. *Chem Commun*, 2011, 47(5): 1384–1404.
- [64] SONG H K, LEE K T, KIM M G, NAZAR L F, CHO J. Recent progress in nanostructured cathode materials for lithium secondary batteries [J]. *Advanced Functional Materials*, 2010, 20(22): 3818–3834.
- [65] JIANG Jian, LI Yuan-yuan, LIU Jin-ping, HUANG Xin-tang, YUAN Chang-zhou, LOU Xiong-wen. Recent advances in metal oxide-based electrode architecture design for electrochemical energy storage [J]. *Advanced Materials*, 2012, 24(38): 5166–5180.

## 正极材料 $\text{LiNi}_x\text{Co}_y\text{Mn}_z\text{O}_2$ 的微/纳结构对 锂离子电池性能改进的最新进展

潘成迟<sup>1</sup>, Craig E. BANKS<sup>2</sup>, 宋维鑫<sup>1</sup>, 王驰伟<sup>3</sup>, 陈启元<sup>1</sup>, 纪效波<sup>1</sup>

1. 中南大学 化学化工学院, 有色金属资源化教育部重点实验室, 长沙 410083;
2. Faculty of Science and Engineering, School of Biology, Chemistry and Health Science, Division of Chemistry and Materials, Manchester Metropolitan University, Chester Street, Manchester M1 5GD, Lancs, UK;
3. 天津市捷威动力工业有限公司, 天津 300380

**摘要:** 微/纳结构  $\text{LiNi}_x\text{Co}_y\text{Mn}_z\text{O}_2$  具有一维、二维、三维形态。综述了其在合成与制备及在锂离子电池应用中的最新进展。掺杂、表面包覆与复合有利于增加电池容量和功率密度, 从而进一步提高其能量效率和比容量, 最终改善其循环稳定性。

**关键词:** 锂离子电池; 微/纳结构;  $\text{LiNi}_x\text{Co}_y\text{Mn}_z\text{O}_2$ ; 掺杂; 表面改性; 复合材料

(Edited by Sai-qian YUAN)